

Published in final edited form as:

*Environ Sci Technol.* 2014 January 7; 48(1): 656–663. doi:10.1021/es404535q.

## Electrolytic Manipulation of Persulfate Reactivity by Iron Electrodes for TCE Degradation in Groundwater

Songhu Yuan<sup>†,‡,\*</sup>, Peng Liao<sup>†</sup>, and Akram N. Alshawabkeh<sup>‡,\*</sup>

<sup>†</sup>State Key Lab of Biogeology and Environmental Geology, China University of Geosciences, 388 Lumo Road, Wuhan, 430074, P. R. China

<sup>‡</sup>Department of Civil and Environmental Engineering, Northeastern University, 400 Snell Engineering, 360 Huntington Avenue, Boston, Massachusetts 02115, United States

### Abstract

Activated persulfate oxidation is an effective in situ chemical oxidation process for groundwater remediation. However, reactivity of persulfate is difficult to manipulate or control in the subsurface causing activation before reaching the contaminated zone and leading to a loss of chemicals. Furthermore, mobilization of heavy metals by the process is a potential risk. An effective approach using iron electrodes is thus developed to manipulate the reactivity of persulfate in situ for trichloroethylene (TCE) degradation in groundwater, and to limit heavy metals mobilization. TCE degradation is quantitatively accelerated or inhibited by adjusting the current applied to the iron electrode, following  $k_1 = 0.00053 \cdot I_v + 0.059$  ( $-122 \text{ A/m}^3 \leq I_v \leq 244 \text{ A/m}^3$ ) where  $k_1$  and  $I_v$  are the pseudo first-order rate constant ( $\text{min}^{-1}$ ) and volume normalized current ( $\text{A/m}^3$ ), respectively. Persulfate is mainly decomposed by  $\text{Fe}^{2+}$  produced from the electrochemical and chemical corrosion of iron followed by the regeneration via  $\text{Fe}^{3+}$  reduction on the cathode.  $\text{SO}_4^{\bullet-}$  and  $\bullet\text{OH}$  co-contribute to TCE degradation, but  $\bullet\text{OH}$  contribution is more significant. Groundwater pH and oxidation-reduction potential can be restored to natural levels by the continuation of electrolysis after the disappearance of contaminants and persulfate, thus decreasing adverse impacts such as the mobility of heavy metals in the subsurface.

### INTRODUCTION

Contamination of groundwater by toxic and persistent organics such as trichloroethylene (TCE) has been a worldwide environmental problem for decades<sup>1,2</sup> and effective remediation is still a challenge. In situ chemical oxidation (ISCO) has developed as a technique of interest because the remediation is fast and relatively cost-effective.<sup>3–5</sup> Oxidants commonly used in ISCO include  $\text{H}_2\text{O}_2$ , permanganate and persulfate.<sup>4</sup>  $\text{H}_2\text{O}_2$  catalyzed by Fe(II) is powerful for organics oxidation;<sup>6,7</sup> but the decomposition of  $\text{H}_2\text{O}_2$  in the subsurface is rapid, resulting in a low utilization efficiency. Permanganate can be consumed by soil organic matter, and its reactivity is limited to alkenes and benzene derivatives containing ring activating groups.<sup>8,9</sup> Persulfate, a relatively newly developed oxidant for use in ISCO, has received more attention because of its potential advantages over  $\text{H}_2\text{O}_2$  and permanganate.<sup>10–18</sup> Persulfate (oxidation potential: 2.01 V, eq. 1) is

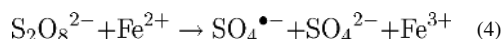
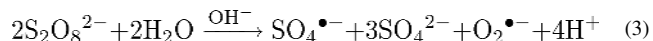
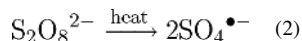
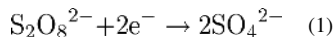
\*To whom correspondence should be addressed: yuansonghu622@hotmail.com (S. Yuan), Phone: +86-27-67848629. Fax: +86-27-67883456; aalsha@coe.neu.edu (A. Alshawabkeh), Phone: 617 373 3994. Fax: 617 373 4419.

The content is solely the responsibility of the authors and does not necessarily represent the official views of the NIEHS or the National Institutes of Health.

Supporting Information Available

Additional descriptions about SI Section S1, Figures S1–9 and Table S1 are provided in SI. This material is available free of charge via the internet at <http://pubs.acs.org>.

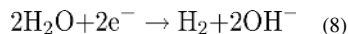
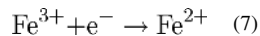
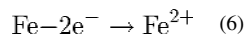
relatively stable due to its slow reaction kinetics with organics;<sup>5</sup> this offers the advantage of effective transport and a larger radius of influence in the subsurface with minimal loss. Upon activation (eqs. 2–5), persulfate can be transformed into powerful oxidizing radicals,  $\text{SO}_4^{\bullet-}$  (oxidation potential: 2.4 V) and  $\bullet\text{OH}$  (oxidation potential: 2.8 V),<sup>5,12</sup> which are able to degrade organics.



For ISCO applications, persulfate is activated mainly by heat, base and transition metals.<sup>5,12</sup> Heating groundwater is energy intensive<sup>19,20</sup> and increasing groundwater pH to above 12 is costly,<sup>21,22</sup> particularly for bicarbonate buffered groundwater. Activation by  $\text{Fe}^{2+}$  is not practical because the reaction is almost instantaneously stalled due to the  $\text{SO}_4^{\bullet-}$  scavenging by excess  $\text{Fe}^{2+}$  or rapid oxidation of  $\text{Fe}^{2+}$  to  $\text{Fe}^{3+}$ .<sup>12</sup>  $\text{Fe}(\text{II})$  chelated by organic acids is effective in activating persulfate,<sup>23–26</sup> but the added organic acids consume more persulfate. It is also environmentally risky to inject chelating agents such as ethylenediamine-tetraacetic acid (EDTA) into the subsurface.<sup>25,26</sup> The significant loss of persulfate due to decomposition before reaching the contaminated zone is a challenge for in situ implementation. Moreover, it is difficult or even impractical to manipulate the reactivity of persulfate in the subsurface for contaminants degradation by activated persulfate after injection of activating agents and persulfate. In addition, the decrease in groundwater pH from persulfate decomposition presents potential risks, including impacting aquifers geochemistry and causing leaching of heavy metals in the subsurface.<sup>4,5</sup> These challenges sometimes lead to inefficient implementation due to the loss of persulfate during transport and injection, uncontrolled reaction rate and potential secondary pollution.

In situ electrolysis by iron electrodes provides options to resolve these challenges: (1) By applying a positive current using an iron anode,  $\text{Fe}^{2+}$  is continuously produced in situ by anodic corrosion (eq. 6).<sup>27,28</sup> When compared with the option of injecting high concentrations of  $\text{Fe}(\text{II})$  solutions,<sup>23–26</sup> the controlled electrolytic supply of  $\text{Fe}^{2+}$  will improve the utilization of both  $\text{Fe}^{2+}$  and persulfate. On the other hand,  $\text{Fe}^{2+}$  production can be suppressed or prevented by reversing polarity (applying a negative current through the iron electrode) due to the cathodic protection effect, thus decreasing or even halting the reactivity of persulfate. As the production rate of  $\text{Fe}^{2+}$  is proportional to the current based on Faraday law, in situ manipulation (i.e., increasing or inhibiting) of persulfate reactivity is theoretically made feasible by adjusting the current. (2) The regeneration of  $\text{Fe}^{2+}$  from  $\text{Fe}^{3+}$  can be enhanced by the reduction of  $\text{Fe}^{3+}$  on the cathode (eq. 7),<sup>29,30</sup> thus further improving the utilization of  $\text{Fe}^{2+}$ .<sup>30,31</sup> (3) Water electrolysis on the cathode produces  $\text{OH}^-$  (eq. 8), which can potentially restore groundwater pH and oxidation-reduction potential (ORP), suppressing the leaching of heavy metals in the subsurface. (4) Iron electrodes can be easily introduced into the contaminated zone to control activation of persulfate in situ, thus

minimizing the potential loss of persulfate during its injection and transport in the subsurface.



We hypothesize that the reactivity of persulfate in the subsurface can be electrolytically manipulated by iron electrodes through quantitatively controlling  $\text{Fe}^{2+}$  supply – and thus persulfate utilization – while inhibiting heavy metals leaching. To justify our hypothesis, this laboratory study investigates the manipulation of persulfate reactivity towards TCE degradation by iron electrodes. TCE is used as the representative of persistent toxic organics because it is frequently detected in contaminated groundwater.<sup>1,2</sup> TCE degradation by persulfate is evaluated by applying different positive and negative currents through the iron electrode serving as anodes and cathodes, respectively. The manipulation is tested by applying different currents during the course of degradation. The relative contributions of different origins of  $\text{Fe}^{2+}$  to persulfate decomposition are investigated. The mechanisms of TCE degradation are elucidated by measuring the radicals and transformation intermediates. Ultimately, restoration of groundwater pH and ORP for inhibiting heavy metal leaching is examined by prolonging electrolysis treatment.

## EXPERIMENTAL SECTION

### Chemicals

TCE (99.5%) was purchased from Sigma-Aldrich. Sodium persulfate (98%) was provided by Alfa. 5,5-Dimethyl-1-pyrroline-N-oxide (DMPO) was from Cayman Chemical Company (USA). Other chemicals include dichloroacetic acid (99%, Fischer Sci.), sodium oxalic (99.8%, J.T Baker), formic acid (88% in water, Acros), tert-butyl-alcohol (TBA, 99%, Fisher Sci.), sodium diethyldithiocarbamate trihydrate (Sigma-Aldrich),  $\text{FeSO}_4 \cdot 7\text{H}_2\text{O}$  (J.T Baker), citric acid (99%, Acros) and gas standard (1% (v/v) methane, ethene, ethane, acetylene,  $\text{CO}_2$  and CO in nitrogen, Supelco). Excess TCE was dissolved into 18.2 m $\Omega$ -cm high-purity water to form a TCE saturated solution (1.07 mg/mL at 20 °C), which was used as the stock solution for preparing aqueous TCE solutions. Deionized water (18.0 M $\Omega$ -cm) obtained from a Millipore Milli-Q system was used in all the experiments. All the other chemicals used in this study were above analytical grade.

### Experimental Procedure

A similar experimental setup as reported previously<sup>32</sup> is used for TCE degradation at ambient temperature. As shown in Figure S1 in the Supporting Information (SI), a 150-mL syringe with a plunger was connected to the cell, allowing gas expansion during electrolysis. Cast gray iron (76 mm length  $\times$  9.5 mm width  $\times$  3.2 mm thickness, MacMaster-Carr, USA) and mixed metal oxide (MMO, 85 mm length  $\times$  15 mm width  $\times$  1.8 mm thickness, IrO<sub>2</sub>/Ta<sub>2</sub>O<sub>5</sub> coating on titanium mesh type, 3N International, USA) were used as the two electrodes in parallel with 42 mm spacing. The overpotential of chlorine evolution on the MMO is measured to be 1.1 V (versus saturated calomel electrode). In a typical test, 390 mL of deionized water was transferred into the cell, 488 mg of sodium persulfate powder was dissolved to obtain an initial concentration of 5 mM, and 20 mL of TCE saturated water was finally added to produce an initial concentration of 0.40 mM (51.2 mg/L). The reactor was

sealed immediately and a constant current was applied. Stirring at 600 rpm was maintained using a Teflon-coated magnetic stirring bar. The solution pH was not controlled during the treatment, showing a quick decrease to about 3 within minutes of the start of the experiments. About 1 mL of aqueous solution was taken out at predetermined time intervals for analysis of TCE and persulfate. The solution was filtrated through a 0.2- $\mu\text{m}$  micropore membrane (Whatman) and was then immediately mixed with 1 mL of methanol to quench further oxidation. Samples were collected for analysis of pH, ORP, total Fe(II) and iron concentrations. All the experiments were carried out at least in duplicate.

A divided electrolytic system was employed to evaluate the relative contributions of (1)  $\text{Fe}^{2+}$  regenerated by  $\text{Fe}^{3+}$  reduction on the MMO cathode and (2) the electrons donated by MMO cathode, to both TCE degradation and persulfate decomposition. The anodic compartment was separated from the cathodic compartment with a Nafion membrane. The solution in the working compartment consisted of 0.40 mM initial TCE concentration and 5 mM initial  $\text{Na}_2\text{S}_2\text{O}_8$  concentration at an initial pH of 5.6, and the solution in the counter compartment consisted of concentrated  $\text{Na}_2\text{SO}_4$  to decrease electric resistance. The reactions in the anodic and cathodic compartments were examined independently. Iron and MMO were used as the anode and cathode, respectively. A constant current of 25 mA was applied.

For analysis of the degradation intermediates, the reactor holding 370 mL of deionized water was purged with He gas for 30 min to remove  $\text{CO}_2$  before addition of the reactants. The initial concentrations of persulfate and TCE were set at 5 and 1.58 mM, respectively. A positive current of +100 mA was applied through the iron anode. 1 mL of aqueous solution was taken out at predetermined time intervals for analysis of TCE, persulfate,  $\text{Cl}^-$  and organic acids.

## Analysis

TCE and persulfate concentrations were measured by a 1200 Infinity Series HPLC (Agilent) equipped with a 1260 DAD detector and a Thermo ODS Hypersil C18 column (4.6  $\times$  50 mm). The mobile phase was a mixture of acetonitrile and water (60:40, v/v) at 1 mL/min. The detection wavelength was 210 nm.  $\text{CO}_2$  was absorbed in NaOH solution and measured for inorganic carbon by the TOC analyzer.<sup>32</sup> Chloride and carboxylic acidic intermediates were analyzed by a Dionex DX-5500 ion chromatograph. Gas concentrations of TCE and aqueous concentration of  $\text{CO}_2$  were calculated by Henry's law, and the sum of aqueous and gas concentrations was derived for mass balance analysis.

The concentration of total ferrous ion was determined at 510 nm using the 1,10-o-phenanthroline analytical method after dissolving the sample in 0.3 M HCl.<sup>33</sup> Total iron concentration was measured after reducing ferric ions to ferrous ions by hydroxylamine hydrochloride. Total ferric concentration is obtained from the difference between total iron concentration and total ferrous ion concentration.  $\text{Cu}^{2+}$  was analyzed at 440 nm after coloration with sodium diethyldithiocarbamate.<sup>33</sup> Radicals generated in the system were assayed by electron spin resonance (ESR). A 100  $\mu\text{L}$  sample was collected from the reactor without addition of contaminants after reacting for 10 min. The sample was immediately mixed with 25  $\mu\text{L}$  of 0.2 M DMPO to form a DMPO-radical adduct, which was then measured on a Bruker EMX ESR spectrum with microwave bridge (receiver gain, 5020; modulation amplitude, 2 Gauss; microwave power, 6.35 mW; modulation frequency, 100 kHz; center field: 3525 G).

## RESULTS AND DISCUSSION

### Effect of Current on TCE Degradation and Persulfate Decomposition

**a) TCE Degradation**—Figure 1a reveals that TCE degradation increases as the current applied through the iron electrode increases from  $-50$  to  $+100$  mA (or from  $-8.7$  to  $17.3$  mA/cm<sup>2</sup>). At  $+100$  mA, more than 99% of TCE is transformed within 20 min in the samples with 0.40 mM initial TCE concentration and 5 mM initial persulfate concentration. Direct mixing of persulfate and TCE in the control experiments produced negligible transformation of TCE. In the absence of persulfate, electrolytic degradation of TCE is minimal within 30 min (SI Figure S2). Therefore, the significant degradation of TCE by persulfate with increasing the current applied through an iron anode can be due to the activation of persulfate by iron electrolysis. TCE degradation is also significant under zero current (0 mA), which is consistent with the literature as zerovalent iron activates persulfate.<sup>34–39</sup> Fitting TCE transformation by pseudo first-order kinetics results in transformation rate constants that increase from  $0.006$  min<sup>-1</sup> at  $-50$  mA to  $0.185$  min<sup>-1</sup> at  $+100$  mA (SI Table S1). A linear correlation between TCE degradation rate constants and applied currents on the iron electrode is determined as:

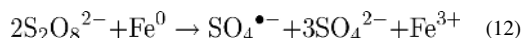
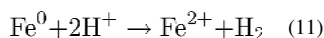
$$k_1 = 0.0013 \bullet I + 0.059 \quad (-50 \text{ mA} \leq I \leq 100 \text{ mA}) \quad R^2 = 0.963 \quad (9)$$

where  $k_1$  and  $I$  are the pseudo first-order degradation constant (min<sup>-1</sup>) and the current (mA), respectively (Figure 1b). To give guidance for practical application, a more generalized relation is derived as eq. 10 by normalizing the current by groundwater volume ( $I_v$ , A/m<sup>3</sup>).

$$k_1 = 0.00053 \bullet I_v + 0.059 \quad (-122 \text{ A/m}^3 \leq I_v \leq 244 \text{ A/m}^3) \quad (10)$$

This suggests that TCE degradation can be quantitatively controlled, i.e., accelerated or inhibited, by adjusting the current applied to the iron electrode. However, this relationship may be affected by the presence of redox-sensitive components (e.g., organic matter, Fe<sup>2+</sup>, Mn<sup>2+</sup>, etc.) in groundwater.<sup>10–12</sup> During the course of degradation, the solution pH decreased to 3.0 due to production of more H<sup>+</sup> from persulfate decomposition and Fe<sup>2/3+</sup> hydrolysis than production of OH<sup>-</sup> at the cathode under all currents,<sup>5,16</sup> and the ORP increased to 520 mV (versus Ag/AgCl) (SI Figure S3).

**b) Persulfate Decomposition**—Figure 1c presents the decomposition of persulfate at different currents with iron electrodes. The decomposition is not significant at currents less than  $-10$  mA, but is enabled as the current increases. The trend is relatively consistent with the degradation of TCE. Theoretically, persulfate decomposes by accepting electrons (eq. 1).<sup>5</sup> In the electrolytic system containing an iron electrode, the electron donors include (1) Fe<sup>2+</sup> produced from the electrochemical corrosion of iron (eq. 6), (2) Fe<sup>2+</sup> produced from the chemical corrosion of iron (eqs. 11 and 12), (3) Fe<sup>2+</sup> regenerated from Fe<sup>3+</sup> reduction on the MMO cathode (eq. 7) and (4) electrons on the cathode surface.



The faster decomposition of persulfate as the current increases confirms the contribution of Fe<sup>2+</sup> produced from the electrochemical corrosion of iron. Likewise, the decomposition of persulfate when no current is applied (0 mA) proves the contribution of Fe<sup>2+</sup> from the

chemical corrosion of iron. The contributions of  $\text{Fe}^{2+}$  regenerated from  $\text{Fe}^{3+}$  reduction on the MMO cathode and of the electrons donated by the MMO cathode are investigated in a divided electrolytic system. Both TCE degradation and persulfate decomposition are significant in the anodic compartment, but are slightly slower than those in the undivided electrolytic system under identical conditions (Figure 2). This further validates the contribution of  $\text{Fe}^{2+}$  produced from the electrochemical corrosion of iron and the limited impact of the cathode reaction. The slight difference reflects the secondary contribution of  $\text{Fe}^{2+}$  regenerated from  $\text{Fe}^{3+}$  reduction on the MMO cathode.<sup>29,30</sup> The regeneration of  $\text{Fe}^{2+}$  from  $\text{Fe}^{3+}$  is effective in the electrolytic system (SI Figure S4). In contrast, both TCE degradation and persulfate decomposition are negligible in the cathodic compartment (Figure 2). Electrochemical measurements also reveal that reduction of persulfate on the iron or MMO cathode is not significant within the range of potentials tested in this study (SI Figure S5). As a consequence, the contribution of electrons donated by the MMO cathode to persulfate decomposition can be precluded. It is thus concluded that persulfate is mainly decomposed by  $\text{Fe}^{2+}$  produced from the electrochemical and chemical corrosion of iron as well as from the reduction of  $\text{Fe}^{3+}$  on the MMO cathode.

To evaluate the relative importance of electrochemical versus chemical corrosion of iron for  $\text{Fe}^{2+}$  production, the production of iron species was measured. As the concentration of total  $\text{Fe}^{2+}$  is below the detection limit (0.03 mg/L) under strongly oxidizing conditions, the production of total iron ions is presented (SI Figure S6a). Iron production increases as the current increases through the iron electrode. The production follows pseudo zero-order kinetics (SI Table S1). The rates of iron production correlates well with the rates of persulfate decomposition ( $R^2 = 0.933$ ,  $-10 \text{ mA} \leq I \leq 100 \text{ mA}$ , Figure 1d), further supporting that the production of iron ions predominantly contributes to persulfate decomposition. The production of iron in the electrolytic system is compared in the tests with and without addition of 5 mM persulfate (SI Figure S7). At  $-50 \text{ mA}$ , production of iron is minimal with or without persulfate. When the current increased to 0 mA, production of iron is significantly enhanced by the addition of persulfate, indicating the predominant contribution of chemical corrosion. Production of  $\text{Fe}^{2+}$  from the chemical corrosion of iron even when it is negatively polarized is reported in our recent investigation.<sup>40</sup> At a higher current of  $+50 \text{ mA}$ , production of iron is slightly enhanced by the addition of persulfate. The slight enhancement suggests that electrochemical corrosion is the predominant mechanism for iron production. As a result, the importance of chemical corrosion declines with increasing the current applied through the iron electrode, while the importance of electrochemical corrosion increases. This conclusion is also supported by the current efficiency for iron production at different currents (SI Figure S6b). The contribution of  $\text{Fe}^{2+}$  regeneration from  $\text{Fe}^{3+}$  reduction on the MMO cathode is also supposed to increase as the current increases because it is an electrochemical reduction, but the importance is minor.

### Electrolytic Manipulation of Persulfate Reactivity for TCE Degradation

As the degradation of TCE is linearly dependent on the current applied through the iron electrode, the reactivity of persulfate towards TCE degradation is manipulated by periodical polarization of the iron electrode. As shown in Figure 3a, TCE degradation is moderate in the first 10 min without polarization ( $k_1 = 0.037 \pm 0.003 \text{ min}^{-1}$ ), decreases when  $-50 \text{ mA}$  is applied in the next 10 min ( $k_1 = 0.015 \pm 0.004 \text{ min}^{-1}$ ), and accelerates when  $+50 \text{ mA}$  is applied in the last 10 min ( $k_1 = 0.105 \pm 0.003 \text{ min}^{-1}$ ). In another test with a different sequence of polarization, TCE degradation is enhanced when  $+50 \text{ mA}$  is applied from 10 to 20 min ( $k_1 = 0.098 \pm 0.003 \text{ min}^{-1}$ ), and is suppressed when  $-50 \text{ mA}$  is applied from 20 to 30 min ( $k_1 = 0.033 \pm 0.003 \text{ min}^{-1}$ ). The significant dependence of persulfate reactivity on the current can be attributed to the current-dependent production of  $\text{Fe}^{2+}$ , which was proven to be responsible for persulfate activation in this system. The slight degradation with the

application of  $-50$  mA current in both sequences is due to the regeneration of  $\text{Fe}^{2+}$  from  $\text{Fe}^{3+}$  reduction on the cathode as well as from the  $\text{Fe}^{3+}$  reduction by intermediates radicals formed by degradation.<sup>26,41</sup> Chlorine evolution may occur in the presence of chloride when the polarity of the MMO is reversed to positive (see anode potentials in SI Table S1). The accumulation of chlorinated organics can be decreased through subsequent degradation when a positive current is applied to the iron electrode.

The decomposition of persulfate is also dependent on the current applied to the iron electrode (Figure 3b). The decomposition is moderate in the first 10 min without polarization ( $k_0 = 0.008 \pm 0.001$  mM/min), nearly stalled by application of  $-50$  mA current from 10 to 20 min ( $k_0 = 0.000 \pm 0.004$  mM/min), and is enhanced by application of  $+50$  mA current from 20 to 30 min ( $k_0 = 0.018 \pm 0.001$  mM/min). In the test with a different sequence of polarization, the decomposition is enhanced by application of  $+50$  mA current from 10 to 20 min ( $k_0 = 0.020 \pm 0.001$  mM/min), and is almost stopped with application of  $-50$  mA current from 20 to 30 min ( $k_0 = 0.002 \pm 0.000$  mM/min). The extremely slow decomposition of persulfate with application of  $-50$  mA indicates that the concentration of persulfate after injection into the subsurface can be artificially maintained when the degradation is not desired. As an important conclusion, it is feasible to electrolytically manipulate both persulfate decomposition and TCE degradation using an iron electrode.

### Mechanisms of TCE Degradation

**a) Radical Scavenging Studies**—For the degradation of organic contaminants by  $\text{Fe}^{2+}$  activated persulfate,  $\text{SO}_4^{\bullet-}$  is generally assumed as the dominant radical.<sup>5,24,42</sup> Nevertheless, the contribution of  $\bullet\text{OH}$  in activated persulfate oxidation has recently been recognized,<sup>20,21,24</sup> and is experimentally validated to be even more pronounced than that of  $\text{SO}_4^{\bullet-}$  for  $\text{Fe}(\text{II})$  activated persulfate.<sup>25</sup> In this study, TBA ( $k_{\bullet\text{OH}} = 6.0 \times 10^8 \text{ M}^{-1} \text{ s}^{-1}$ ,  $k_{\text{SO}_4^{\bullet-}} = 4.0 \times 10^5 \text{ M}^{-1} \text{ s}^{-1}$ ) and methanol ( $k_{\bullet\text{OH}} = 9.7 \times 10^8 \text{ M}^{-1} \text{ s}^{-1}$ ,  $k_{\text{SO}_4^{\bullet-}} = 3.2 \times 10^6 \text{ M}^{-1} \text{ s}^{-1}$ ) are used to evaluate the relative contribution of  $\text{SO}_4^{\bullet-}$  and  $\bullet\text{OH}$  because of their different reaction rates.<sup>10,17,20,43</sup> Figure 4a shows that TCE degradation is markedly inhibited by the addition of 60 mM TBA, and the inhibition slightly increases by the addition of 300 mM TBA. This implies that 300 mM TBA is sufficient to scavenge  $\bullet\text{OH}$ . The rate constants of TCE degradation without scavenging agents and with 300 mM TBA are  $0.125 \pm 0.010$  and  $0.039 \pm 0.003 \text{ min}^{-1}$ , respectively. Thus, the relative contribution of  $\bullet\text{OH}$  is calculated to be 68.8% (SI Section S1). By the addition of 60 mM methanol, the inhibition is similar with that of TBA. However, the addition of 300 mM methanol increases the inhibition, decreasing the rate constant to  $0.026 \pm 0.003 \text{ min}^{-1}$ . The difference between the inhibition by the addition of TBA and methanol can be attributed to the contribution of  $\text{SO}_4^{\bullet-}$ . The relative contribution of  $\text{SO}_4^{\bullet-}$  is calculated to be 10.4% (SI Section S1). This suggests that  $\bullet\text{OH}$  produced from  $\text{SO}_4^{\bullet-}$  (eq. 5) plays a much more important role than  $\text{SO}_4^{\bullet-}$  for TCE degradation, which agrees with recent findings in literature.<sup>20,25</sup> The sum of contributions of  $\bullet\text{OH}$  and  $\text{SO}_4^{\bullet-}$  is less than 100%, suggesting the involvement of other degradation pathways which are not identified.

**b) ESR Studies**—The radicals are further measured by ESR assay. Figure 4b reveals that the signals for the combination of persulfate and iron anode at  $+50$  mA are much higher than the signals for each independently. The characteristic 1:2:2:1 spectrum of  $\text{DMPO}/\bullet\text{OH}$  adduct with hyperfine coupling constants of  $a_{\text{N}} = 14.9 \text{ G}$  and  $a_{\text{H}} = 14.9 \text{ G}$  is clearly observed,<sup>10,25,44</sup> validating the production of  $\bullet\text{OH}$ . A  $\text{DMPO}/\text{SO}_4^{\bullet-}$  adduct with hyperfine splitting constants of  $a_{\text{N}} = 13.3$ ,  $a_{\text{H}} = 9.3$ ,  $a_{\text{H}} = 1.3$ , and  $a_{\text{H}} = 0.8 \text{ G}$ <sup>10,21,25</sup> also appear but shows much lower intensity compared with  $\text{DMPO}/\bullet\text{OH}$ . The ESR spectrums coincide with those reported.<sup>10,21,25</sup> ESR results further support that  $\text{SO}_4^{\bullet-}$  and  $\bullet\text{OH}$  are the oxidizing radicals responsible for TCE degradation.

**c) Evolution of Degradation Intermediates**—Degradation of TCE by activated persulfate is evaluated by the concentration decrease in previous studies,<sup>10,11,19,22,25</sup> which neglects the fate of TCE and the potential risk of degradation intermediates. In this study, the evolution of degradation intermediates was quantified, demonstrating the accumulation of organic acids intermediates aside from the mineralization product of CO<sub>2</sub> (Figure 4c). The mass balances for carbon and chlorine indicate nearly complete recovery of carbon and chlorine in these intermediates. Waldemer et al. recovered 80–90% chloride for oxidation of TCE by SO<sub>4</sub><sup>•-</sup> produced from heat-activated persulfate, but did not present the quantitative evolution of degradation intermediates.<sup>19</sup> Different organic acids are measured for the oxidation of TCE by •OH produced from Fenton-based processes depending on the reaction conditions.<sup>32,45</sup> A simple comparison of intermediates formation is difficult because of limited data available on the intermediates from persulfate oxidation of TCE. The intermediates accumulated herein are similar but not identical to those reported for the oxidation by •OH produced from Fenton-based processes.<sup>32,45</sup> The difference can be attributed to the contribution of SO<sub>4</sub><sup>•-</sup> in addition to •OH. In general, SO<sub>4</sub><sup>•-</sup> is more selective for electron transfer reactions than •OH which can rapidly undergo reaction by hydrogen abstraction or addition.<sup>22,41,46</sup> Note that dichloroacetic acid, a likely human carcinogen,<sup>47</sup> accumulated significantly; a longer degradation time is necessary for its elimination even though TCE will have been completely removed. As such, application of activated persulfate oxidation of TCE in groundwater should be carefully monitored to ensure complete degradation of transformation byproducts.

### Inhibition of Heavy Metal Mobilization

To test the mobility of heavy metals during treatment, 10 mg/L Cu<sup>2+</sup> was added to the solution. For the case of transformation of 0.40 mM TCE by 2 mM persulfate at +100 mA, Figure 5a shows that the solution pH and ORP are maintained at about 3.2 and 450 mV (versus Ag/AgCl), respectively, within 45 min before the disappearance of TCE and persulfate. In this stage, Cu<sup>2+</sup> concentration is about 9 mg/L (Figure 5b), implying a strong mobility potential. After 45 min of electrolysis and the disappearance of TCE and persulfate, a continuation of the electrolysis produces sufficient Fe<sup>2+</sup> for persulfate decomposition (eq. 6), and the simultaneous production of OH<sup>-</sup> from the cathode (eq. 8) neutralizes the acidity. Production of Fe<sup>2+</sup> decreases ORP but increases pH through hydrolysis, while production of OH<sup>-</sup> increases pH. The incomplete hydrolysis of Fe<sup>2+</sup> ( $pK_{sp, Fe(OH)_2} = 16.31$ ) implies the excess of OH<sup>-</sup> for pH increase. As a consequence, the solution ORP quickly drops to -60 mV (versus Ag/AgCl), and the solution pH quickly increases to 7 after 45 min (Figure 5a). The concentration of Cu<sup>2+</sup> decreases to a low level of 0.17 mg/L (Figure 4b) due to precipitation by OH<sup>-</sup> and adsorption by Fe-hydroxides under neutral conditions. Therefore, continuing the electrolysis after disappearance of contaminants and persulfate provides an effective approach to restoring groundwater chemistry, i.e., pH and ORP, thus inhibiting the mobilization of cationic metals. In addition, under the developed Fe(II)-rich conditions, many toxic anionic metals such as chromium, arsenic, selenium, and uranium can be immobilized as well.<sup>48,49</sup> Nonetheless, metals may be mobilized away from the electrodes prior to pH restoration when groundwater flows at a high rate. In this case, periodical treatment with injection of low concentrations of persulfate is necessary to inhibit metal mobilization.

### Implications

The manipulation of persulfate reactivity for TCE degradation is achieved by adjusting the current applied to an iron electrode. Fe<sup>2+</sup> produced from the iron decomposes and activates persulfate producing strongly oxidizing SO<sub>4</sub><sup>•-</sup> and •OH radicals, thus degrading TCE. Compared with the activation by citrate chelated Fe<sup>2+</sup>, this new means of activation achieves similar efficiency for TCE degradation (SI Figure S8). Although iron anode activation



consumes electricity to reach similar efficiency, it would be feasible to control the rate of contaminant degradation when applied in situ. Compared with existing activation methods, the new activation method developed in this study has the potential advantage of restoring groundwater pH and ORP to natural levels and reducing the risk of heavy metal mobilization.

In situ manipulation of persulfate reactivity can be efficiently achieved by inserting iron electrodes into wells in the contaminated zone. The conceptual model of the manipulation is illustrated in SI Figure S9. Except persulfate, the activating ( $\text{Fe}^{2+}$ ) and other ( $\text{OH}^-$ ) chemicals are all produced in situ. Notably, the presence of chloride and bicarbonate in groundwater may affect the efficiency because both anions compete with contaminants for the oxidizing radicals, and bicarbonate buffers pH variation.<sup>19,50</sup> Groundwater background components such as organic matter,  $\text{Fe}^{2+}$  and  $\text{Mn}^{2+}$  may inevitably contribute to persulfate activation, thereby decreasing the effectiveness of electrolytic manipulation. As the co-transport of  $\text{Fe}^{2+}$  with persulfate in the subsurface is difficult, the radius of influence of this new activation method is another challenge, which needs further investigation.

## Supplementary Material

Refer to Web version on PubMed Central for supplementary material.

## Acknowledgments

This work was supported by the National Institute of Environmental Health Sciences (NIEHS, Grant No. P42ES017198), the National Science Foundation of China (NSFC, No. 21277129) and State Key Laboratory of Biogeology and Environmental Geology, China University of Geosciences (No. GBL11204). We appreciate the assistance in ESR assay by Prof. David Budil and Mr. Xianzhe Wang in Department of Chemistry & Chemical Biology, Northeastern University.

## References

1. Moran MJ, Zogorski JS, Squillage PJ. Chlorinated solvents in groundwater of the United States. *Environ Sci Technol.* 2007; 41:74–81. [PubMed: 17265929]
2. Stroo HF, Leeson A, Marqusee JA, Johnson PC, Ward CH, Kavanaugh MC, Sale TC, Newell CJ, Pennell KD, Lebrón CA, Unger M. Chlorinated ethene source remediation: Lessons learned. *Environ Sci Technol.* 2012; 46:6438–6447. [PubMed: 22558915]
3. Watts RJ, Teel AL. Treatment of contaminated soils and groundwater using ISCO. *Pract Period Hazard, Toxic, Radioact Waste Manage.* 2006; 10:2–9.
4. ITRC. Technical and Regulatory Guidance for In Situ Chemical Oxidation of Contaminated Soil and Groundwater. ITRC, ISCO Team; Washington, DC: 2005.
5. Tsitonaki A, Petri B, Crimi M, Mosbaek H, Siegrist RL, Bjerg PL. In situ chemical oxidation of contaminated soil and groundwater using persulfate: A review. *Crit Rev Environ Sci Technol.* 2010; 40:55–91.
6. Navalon S, Alvaro M, Garcia H. Heterogeneous Fenton catalysts based on clays, silicas and zeolites. *Appl Catal B Environ.* 2010; 99:1–26.
7. Ravikumar JX, Gurol MD. Chemical oxidation of chlorinated organics by hydrogen peroxide in the presence of sand. *Environ Sci Technol.* 1994; 28:394–400. [PubMed: 22165872]
8. Gates-Anderson DD, Siegrist RL, Cline SR. Comparison of potassium permanganate and hydrogen peroxide as chemical oxidants for organically contaminated soils. *J Environ Eng ASCE.* 2001; 127:337–347.
9. Huang KC, Hoag GE, Chheda P, Woody BA, Dobbs GM. Chemical oxidation of trichloroethylene with potassium permanganate in a porous medium. *Adv Environ Res.* 2002; 7:217–229.
10. Fang GD, Gao J, Dionysiou DD, Liu C, Zhou DM. Activation of persulfate by quinones: Free radical reactions and implications for the degradation of PCBs. *Environ Sci Technol.* 2013; 47:4605–4611. [PubMed: 23586773]

11. Ahmad M, Teel AL, Watts RJ. Mechanism of persulfate activation by phenols. *Environ Sci Technol.* 2013; 47:5865–5871.
12. Liang CJ, Bruell CJ, Marley MC, Sperry KL. Persulfate oxidation for in situ remediation of TCE. I. Activated by ferrous ion with and without a persulfate-thiosulfate redox couple. *Chemosphere.* 2004; 55:1213–1223. [PubMed: 15081762]
13. Liang CJ, Lee IL. In situ iron activated persulfate oxidative fluid sparging treatment of TCE contamination—A proof of concept study. *J Contam Hydrol.* 2008; 100:91–100. [PubMed: 18649972]
14. Bennedsen LR, Muff J, Søgaaard EG. Influence of chloride and carbonates on the reactivity of activated persulfate. *Chemosphere.* 2012; 86:1092–1097. [PubMed: 22217455]
15. Yen CH, Chen KF, Kao CM, Liang SH, Chen TY. Application of persulfate to remediate petroleum hydrocarbon-contaminated soil: Feasibility and comparison with common oxidants. *J Hazard Mater.* 2011; 186:2097–2102. [PubMed: 21255917]
16. House DA. Kinetics and mechanism of oxidations by peroxydisulfate. *Chem Rev.* 1962; 62:185–203.
17. Zhang T, Zhu HB, Croué JP. Production of sulfate radical from peroxymonosulfate induced by a magnetically separable  $\text{CuFe}_2\text{O}_4$  spinel in water: Efficiency, stability and mechanism. *Environ Sci Technol.* 2013; 47:2784–2791. [PubMed: 23439015]
18. Drzewicz P, Perez-Estrada L, Alpatova A, Martin JW, El-Din MG. Impact of peroxydisulfate in the presence of zero valent iron on the oxidation of cyclohexanoic acid and naphthenic acids from oil sands process-affected water. *Environ Sci Technol.* 2012; 46:8984–8991. [PubMed: 22799739]
19. Waldemer RH, Tratnyek PG, Johnson RL, Nurmi JT. Oxidation of chlorinated ethenes by heat-activated persulfate: Kinetics and products. *Environ Sci Technol.* 2007; 41:1010–1015. [PubMed: 17328217]
20. Liang CJ, Su HW. Identification of sulfate and hydroxyl radicals in thermally activated persulfate. *Ind Eng Chem Res.* 2009; 48:5558–5562.
21. Furman O, Teel AL, Watts RJ. Mechanism of base activation of persulfate. *Environ Sci Technol.* 2010; 44:6423–6428. [PubMed: 20704244]
22. Liang C, Wang ZS, Bruell CJ. Influence of pH on persulfate oxidation of TCE at ambient temperatures. *Chemosphere.* 2007; 66:106–113. [PubMed: 16814844]
23. Liang CJ, Bruell CJ, Marley MC, Sperry KL. Persulfate oxidation for in situ remediation of TCE. II. Activated by chelated ferrous ion. *Chemosphere.* 2004; 55:1225–1233. [PubMed: 15081763]
24. Rastogi A, Al-Abed SR, Dionysiou DD. Sulfate radical-based ferrous-peroxymonosulfate oxidative system for PCBs degradation in aqueous and sediment systems. *Appl Catal B Environ.* 2009; 85:171–179.
25. Ahmad M, Teel AL, Furman OS, Reed JI, Watts RJ. Oxidative and reductive pathways in iron-ethylenediaminetetraacetic acid-activated persulfate systems. *J Environ Eng ASCE.* 2012; 138:411–418.
26. Liang CJ, Liang CP, Chen CC. pH dependence of persulfate activation by EDTA/Fe(III) for degradation of trichloroethylene. *J Contam Hydrol.* 2009; 106:173–182. [PubMed: 19286273]
27. Mao XH, Ciblak A, Amiri M, Alshawabkeh AN. Redox control for electrochemical dechlorination of trichloroethylene in bicarbonate aqueous media. *Environ Sci Technol.* 2011; 46:3398–3405. [PubMed: 22315993]
28. Wang YR, Chu W. Degradation of 2,4,5-trichlorophenoxyacetic acid by a novel electro-Fe(II)/oxone process using iron sheet as the sacrificial anode. *Water Res.* 2011; 45:3883–3889. [PubMed: 21550624]
29. Brillas E, Sirés I, Oturan A. Electro-Fenton process and related electrochemical technologies based on Fenton's reaction chemistry. *Chem Rev.* 2009; 109:6570–6631. [PubMed: 19839579]
30. Lin H, Wu J, Zhang H. Degradation of bisphenol A in aqueous solution by a novel electro/Fe<sup>3+</sup>/ peroxydisulfate process. *Sep Purif Technol.* 2013; 117:18–23.
31. Zou J, Ma J, Chen LW, Li XC, Guan YH, Xie PC, Pan C. Rapid acceleration of ferrous iron/ peroxymonosulfate oxidation of organic pollutants by promoting Fe(III)/Fe(II) cycle with hydroxylamine. *Environ Sci Technol.* 2013 DOI: dx.doi.org/10.1021/es4019145.

32. Yuan SH, Mao X, Alshawabkeh AN. Efficient degradation of TCE in groundwater using Pd and electro-generated H<sub>2</sub> and O<sub>2</sub>: A shift in pathway from hydrodechlorination to oxidation in the presence of ferrous ions. *Environ Sci Technol*. 2012; 46:3398–3405. [PubMed: 22315993]
33. State Environmental Protection Administration. *Water and Wastewater Monitoring and Analytic Methods*. 4. China Environmental Science Press; Beijing: 2002.
34. Liang C, Lai MC. Trichloroethylene degradation by zero valent iron activated persulfate oxidation. *Environ Eng Sci*. 2008; 25:1071–1078.
35. Liang CJ, Guo YY. Mass transfer and chemical oxidation of naphthalene particles with zerovalent iron activated persulfate. *Environ Sci Technol*. 2010; 44:8203–8208. [PubMed: 20879763]
36. Oh SY, Kim HW, Park JM, Park HS, Yoon C. Oxidation of polyvinyl alcohol by persulfate activated with heat, Fe<sup>2+</sup>, and zero-valent iron. *J Hazard Mater*. 2009; 168:346–351. [PubMed: 19285795]
37. Oh SK, Kang SG, Chiu PC. Degradation of 2,4-dinitrotoluene by persulfate activated with zerovalent iron. *Sci Total Environ*. 2010; 408:3464–3468. [PubMed: 20471066]
38. Ahn S, Peterson TD, Righter J, Miles DM, Tratnyek PG. Disinfection of ballast water with iron activated persulfate. *Environ Sci Technol*. 2013 DOI: dx.doi.org/10.1021/es402508k.
39. Zhu LL, Ai Z, Ho W, Zhang LZ. Core-shell Fe-Fe<sub>2</sub>O<sub>3</sub> nanostructures as effective persulfate activator for degradation of methyl orange. *Sep Purif Technol*. 2013; 108:159–165.
40. Liao P, Yuan SH, Chen MJ, Tong M, Xie WJ, Zhang P. Regulation of electrochemically generated ferrous ions from an iron cathode for Pd-catalytic transformation of MTBE in Groundwater. *Environ Sci Technol*. 2013; 47:7918–7926. [PubMed: 23768068]
41. Minisci C. Electron-transfer processes: Peroxydisulfate, a useful and versatile reagent in organic chemistry. *Accounts Chem Res*. 1983; 16:27–32.
42. Kolthoff IM, Medalia AI, Raaen HP. The reaction between ferrous iron and peroxides. IV. Reaction with potassium persulfate. *J Am Chem Soc*. 1951; 73:1733–1739.
43. Guan YH, Ma J, Li XC, Fang JY, Chen LW. Influence of pH on the formation of sulfate and hydroxyl radicals in the UV/peroxymonosulfate system. *Environ Sci Technol*. 2011; 45:9308–9314. [PubMed: 21999357]
44. Rangelova K, Rice AB, Khajo A, Triquigneaux M, Garantziotis S, Magliozzo RS, Mason RP. Formation of reactive sulfite-derived free radicals by the activation of human neutrophils: An ESR study. *Free Radical Biol Med*. 2012; 52:1264–1271. [PubMed: 22326772]
45. Pham HT, Kitsuneduka M, Hara J, Suto K, Inoue C. Trichloroethylene transformation by natural mineral pyrite: The deciding role of oxygen. *Environ Sci Technol*. 2008; 42:7470–7475. [PubMed: 18939588]
46. Madhavan V, Levanon H, Neta P. Decarboxylation by SO<sub>4</sub><sup>•-</sup> radicals. *Radiat Res*. 1978; 76:15–22.
47. USEPA. Toxicological review of dichloroacetic acid. 2003. EPA 635/R-03/007
48. Mao XH, Yuan SH, Fallahpour N, Ciblak A, Howard J, Padilla I, Loch-Carusio R, Alshawabkeh AN. Electrochemically induced dual reactive barriers for transformation of TCE and mixture of contaminants in groundwater. *Environ Sci Technol*. 2012; 46:12003–12011. [PubMed: 23067023]
49. Stewart BD, Nico PS, Fendorf S. Stability of uranium incorporated into Fe (hydr)oxides under fluctuating redox conditions. *Environ Sci Technol*. 2009; 43:4922–4927. [PubMed: 19673286]
50. Fang GD, Dionysiou DD, Wang Y, Al-Abed SR, Zhou DM. Sulfate radical based degradation of polychlorinated biphenyls: Effects of chloride ion and reaction kinetics. *J Hazard Mater*. 2012; 227–228:394–401.

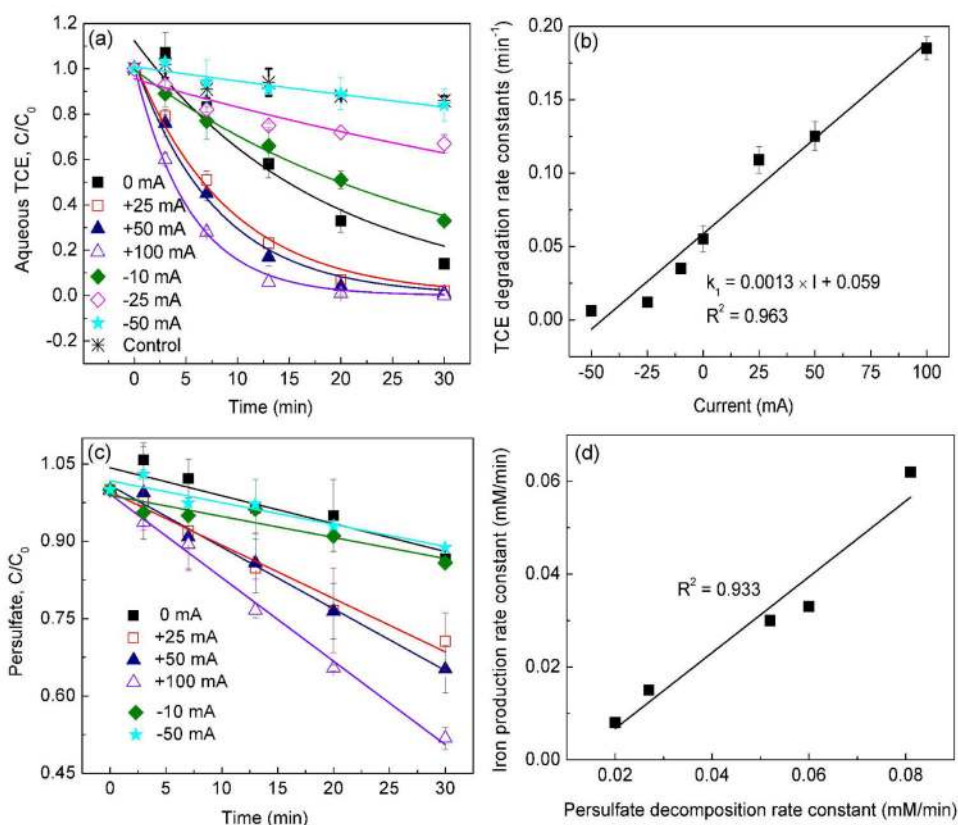


**Figure 1.** Effect of applied current through iron electrodes on (a) TCE degradation and (c) persulfate decomposition; correlation of (b) TCE degradation rate constants on current and (d) iron production rate constants on persulfate decomposition rate constants. Unless otherwise specified, the reaction conditions are based on 0.40 mM initial TCE concentration, 5 mM initial  $\text{Na}_2\text{S}_2\text{O}_8$  concentration and initial pH of 5.6. Solution pH decreases to about 3 during treatment. The curves and lines in (a) and (c) refer to the fittings by pseudo first-order and pseudo zero-order kinetics for the data points in the same color, respectively.

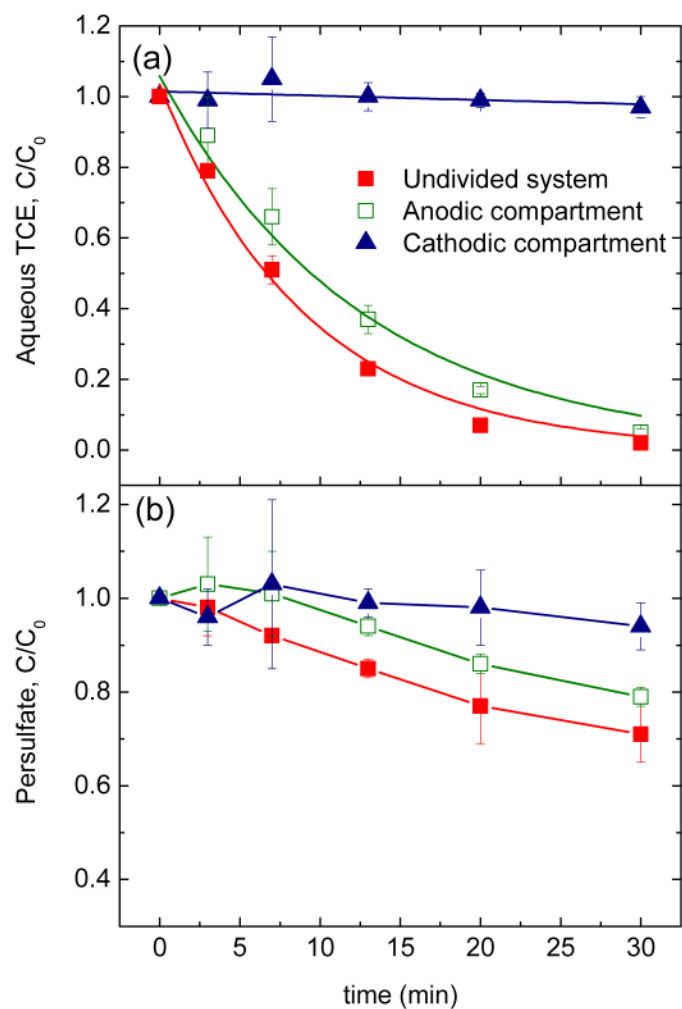


**Figure 2.** Variations of (a) TCE and (b) persulfate concentrations in a divided electrolytic system. The reaction conditions are based on 25 mA, 0.40 mM initial TCE concentration, 5 mM initial  $\text{Na}_2\text{S}_2\text{O}_8$  concentration and initial pH of 5.6. The curves in (a) refer to the fittings by pseudo first-order kinetics for the data points in the same color, respectively.

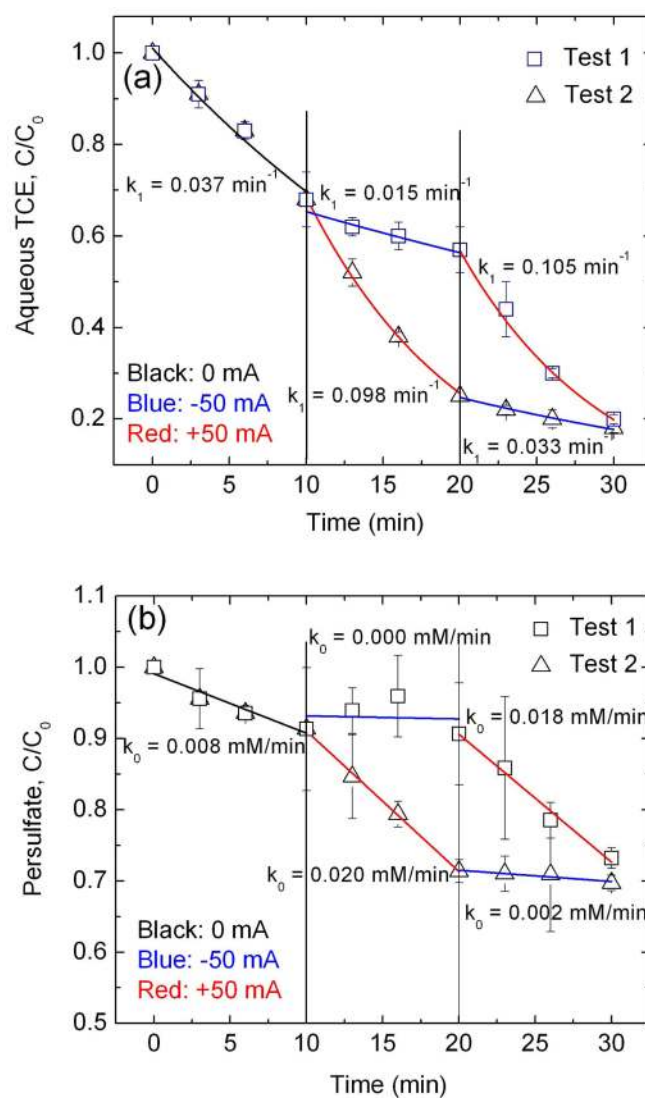


**Figure 3.** Electrolytic manipulation of (a) TCE degradation and (b) persulfate decomposition by periodically applying different currents. Unless otherwise specified, the reaction conditions are based on 0.79 mM initial TCE concentration, 5 mM initial  $\text{Na}_2\text{S}_2\text{O}_8$  concentration and initial pH of 5.6. Note that a higher initial concentration of TCE is used to attain pronounced variation of degradation rates in each stage. Solution pH decreases to about 3 during treatment.  $k_1$  and  $k_0$  refers to the pseudo first-order rate constants of TCE degradation and pseudo zero-order rate constants of persulfate decomposition, respectively. The curves and lines in (a) and (b) refer to the fittings by pseudo first-order and pseudo zero-order kinetics for the data points in the same color, respectively.

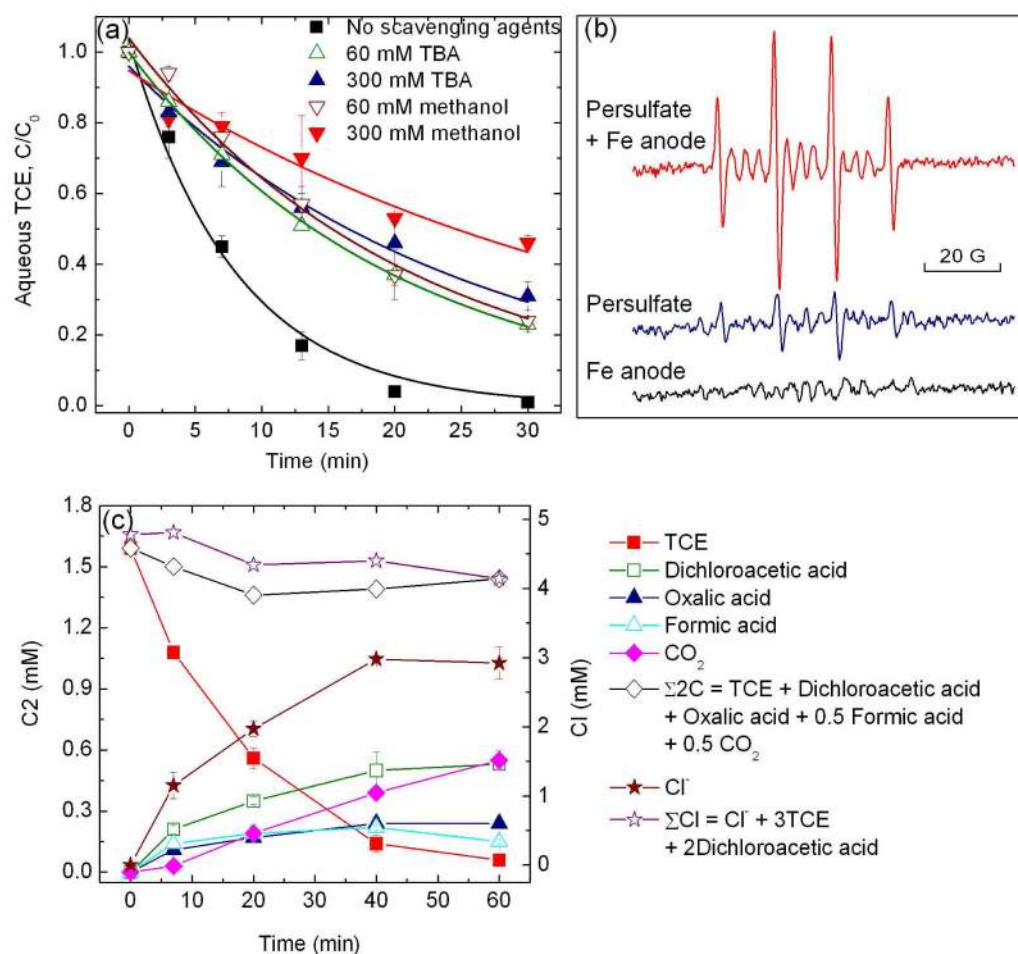


**Figure 4.**

(a) Effect of radical scavenging agents on TCE degradation. The reaction conditions are based on 5 mM initial  $\text{Na}_2\text{S}_2\text{O}_8$  concentration, 0.40 mM TCE, +50 mA on the iron anode and initial pH of 5.6. The curves refer to the fittings by pseudo first-order kinetics for the data points in the same color. (b) ESR signals for iron anode activated persulfate oxidation. The reaction conditions are based on 5 mM initial  $\text{Na}_2\text{S}_2\text{O}_8$  concentration, +50 mA on the iron anode and initial pH of 5.6. The samples were taken at 10 min. (c) Profile of TCE degradation. The reaction conditions are based on 5 mM initial  $\text{Na}_2\text{S}_2\text{O}_8$  concentration, 1.58 mM TCE, +100 mA on the iron anode and initial pH of 5.6.

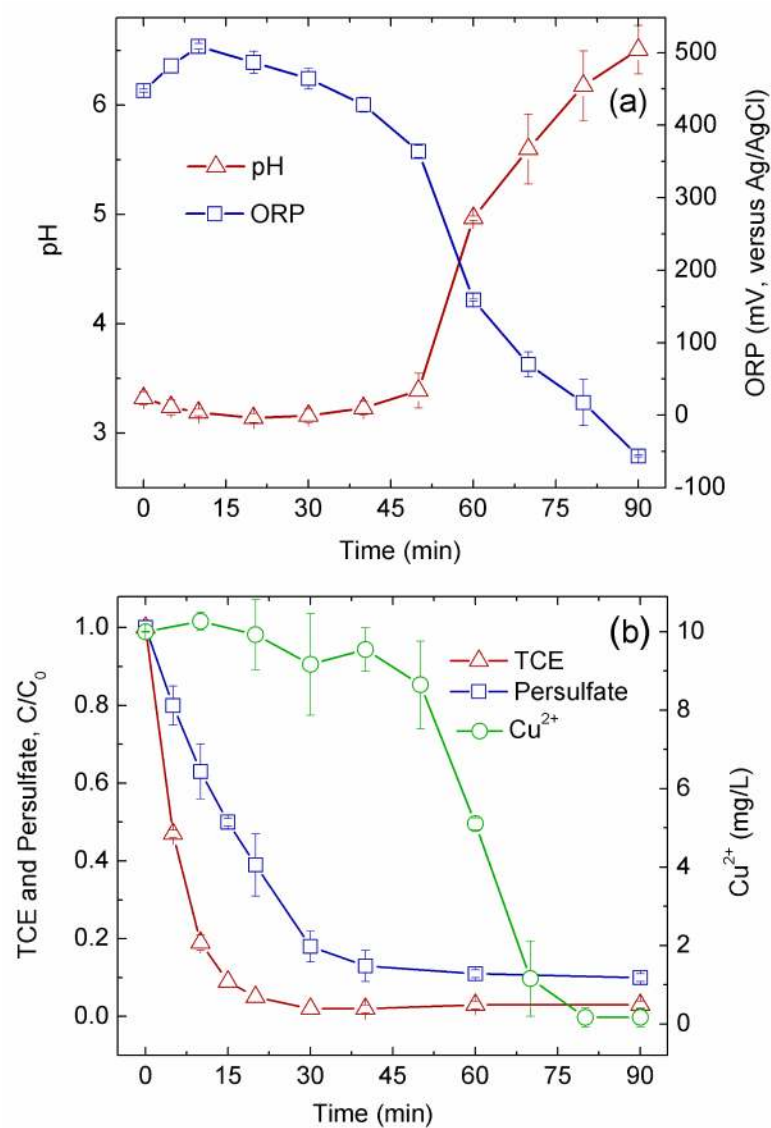


**Figure 5.** Variations of (a) pH/ORP and (b) TCE, persulfate and free Cu<sup>2+</sup> concentrations during the course of treatment. The reaction conditions are based on 0.40 mM initial TCE concentration, 2 mM Na<sub>2</sub>S<sub>2</sub>O<sub>8</sub>, 10 mg/L Cu<sup>2+</sup>, and +100 mA on the iron anode.